Molecular Crystals and Liquid Crystals
Publication details, including instructions for authors and subscription information:
http://www.tandfonline.com/loi/gmcl16

The Metabolemeter IV-Phase Transitions of Binary Mixtures of Mesogens Detected on About One Milligram Samples

J. M. Buisine [a] & J. Billard [b]

[a] Equipe de Dynamique des Cristaux Moléculaires Université des Sciences et Techniques de Lille, 59650, Villeneuve D'asc, France

[b] Laboratoire de Physique de la Matière Collége de France, 75231, Paris, Cedex 05, France

Version of record first published: 17 Oct 2011.

To cite this article: J. M. Buisine & J. Billard (1985): The Metabolemeter IV-Phase Transitions of Binary Mixtures of Mesogens Detected on About One Milligram Samples, Molecular Crystals and Liquid Crystals, 127:1, 353-379

To link to this article: http://dx.doi.org/10.1080/00268948508080851

Mol. Cryst. Liq. Cryst., 1985, Vol. 127, pp. 353–379
0026-8941/85/1274–0353/$25.00/0

Printed in the United States of America

The Metabolemeter IV-Phase Transitions of Binary Mixtures of Mesogens Detected on About One Milligram Samples.†

J. M. BUISINE

Equipe de Dynamique des Cristaux Moléculaires Université des Sciences et Techniques de Lille, 59650 Villeneuve D'asc—France

and

J. BILLARD

Laboratoire de Physique de la Matière Condensée Collège de France, 75231—Paris Cedex 05–France

Equipes de recherches associées au C.N.R.S.

(*Received July 19, 1984*)

For perfect solutions, thermobarograms for binary mixtures of mesogens enclosed in a metallic cell can be calculated. Experimental tests are performed with the metabolemeter on two mixtures of 4-methoxy-4′-ethyltolane and 4-methoxy-4′-n-nonyltolane using about one milligram samples. The experimental thermobarograms agree with calculations and allow very easily the detection of all the transformations. Moreover, for pure 4-methoxy-4′-ethyltolane, the volume change for the virtual nematic-liquid transition can be deduced. The method is then used to determine the (1-methyl)-heptyl terephthalidene bis amino cinnamate and bis-4-n-heptoloxybenzylidene phenylene amine phase diagram; the microscopic observations about the existence of a mesophase which doesn't exist for pure compounds are considered; the concentration existence domain of that mesophase is determined.

†Paper presented at the 10th International Liquid Crystal Conference, York, 15–21 July 1984.

1. INTRODUCTION

The efficiency of the metabolemeter to detect first and second order phase transitions, to draw pressure-temperature phase diagrams of pure mesogens[1-3] and to detect under pressure the glass transition of polymers[4] has been previously shown. Now we use this apparatus to study phase transitions of binary mixtures of mesogens in order to build isobaric phase diagrams useful for identifying mesophases by the miscibility method, to characterize virtual transitions, and then to examine the existence of an intermediary phase which doesn't exist for pure compounds.

2. PRINCIPLE OF THE METHOD

For pure compounds, first and second order phase transitions[1,3] and glass transitions[4] can be detected by the measurement, versus temperature, of the pressure of a sample enclosed in a metallic cell. The simultaneous recording of both data gives thermobarograms. Very small samples (less than one milligram) can be used.[2]

3. THERMOBAROGRAMS FOR BINARY MIXTURES

Here we consider, for a binary mixture of two mesogens A and B of concentration C, exhibiting successively a crystalline phase (K) and two fluid phases (e.g., a mesophase (M) and an isotrope liquid phase (I)) (Figure 1), first, the drawing of the thermobarograms for the different transformations, and second, the order of magnitude of the observed phenomena[5].

General relations

For two perfect solutions 1 and 2 of two compounds in equilibrium, the relations between the mole fraction χ, temperature T and pressure P are connected by the Nernst relations.

$$d\ln\left(\frac{\chi_A^1}{\chi_A^2}\right) = -\frac{\Delta\mathcal{H}_A}{RT^2}dT + \frac{\Delta\mathcal{V}_A}{RT}dP$$
$$d\ln\left(\frac{\chi_B^1}{\chi_B^2}\right) = -\frac{\Delta\mathcal{H}_B}{RT^2}dT + \frac{\Delta\mathcal{V}_B}{RT}dP \qquad (1)$$

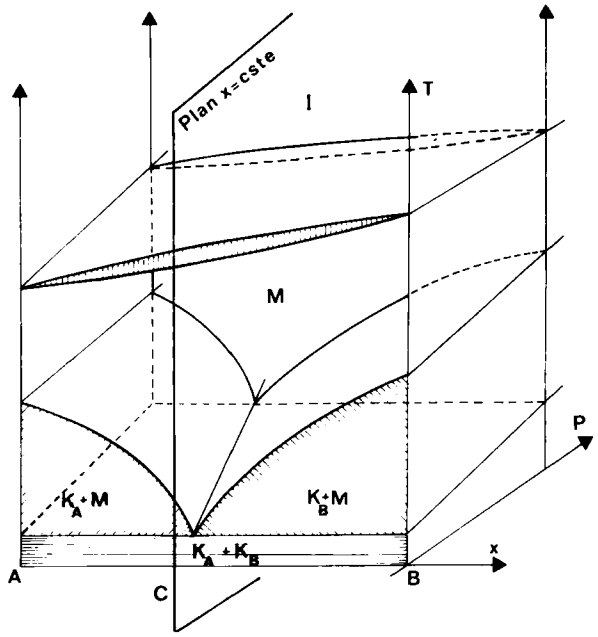

FIGURE 1 Simple tridimensional phase diagram of condensed phases of a binary mixture: x composition, P pressure, T temperature.

where $\Delta\mathscr{H}_A$ and $\Delta\mathscr{H}_B$, $\Delta\mathscr{V}_A$ and $\Delta\mathscr{V}_B$ are respectively the molar enthalpy and volume changes of pure compounds A and B at the 1–2 transition, and R is the gas constant. The volume of the mixture is:

$$V = n_A^1 \mathscr{V}_A^1 + n_A^2 \mathscr{V}_A^2 + n_B^1 \mathscr{V}_B^1 + n_B^2 \mathscr{V}_B^2$$

if $\mathscr{V}_A^1, \mathscr{V}_A^2, \mathscr{V}_B^1, \mathscr{V}_B^2$ and $n_A^1, n_A^2, n_B^1, n_B^2$ are respectively the molar volumes and numbers of moles of both compounds A and B in the 1 and 2 solutions. The volume V can be expressed versus the mole fractions:

$$V = \frac{n}{\chi_A^1 - \chi_A^2}\left[\chi_A^1(C - \chi_A^2)\mathscr{V}_A^1 + \chi_A^2(\chi_A^1 - C)\mathscr{V}_A^2 + (1 - \chi_A^1)(C - \chi_A^2)\mathscr{V}_B^1 + (1 - \chi_A^2)(\chi_A^1 - C)\mathscr{V}_B^2\right]$$

with n the total number of moles in the mixture and C the concentration of A in the sample. For two perfect solutions in equilibrium and

a temperature change dT the mole fractions and pressure changes $d\chi_A^1, d\chi_A^2$ and dP and the volume variation dV are connected by:

$$dV = n\left[C\alpha_A^1\mathscr{V}_A^1 + (1-C)\alpha_B^1\mathscr{V}_B^1\right]dT$$
$$-n\left[C\chi_A^1\mathscr{V}_A^1 + (1-C)\chi_B^1\mathscr{V}_B^1\right]dP$$
$$+\frac{n(C-\chi_A^2)}{(\chi_A^1-\chi_A^2)^2}\left[\chi_A^2\Delta\mathscr{V}_A + (1-\chi_A^2)\Delta\mathscr{V}_B\right]d\chi_A^1$$
$$-\frac{n(C-\chi_A^1)}{(\chi_A^1-\chi_A^2)^2}\left[\chi_A^1\Delta\mathscr{V}_A + (1-\chi_A^1)\Delta\mathscr{V}_B\right]d\chi_A^2 \qquad (2)$$

In that relation, the temperature and pressure dependence of $\Delta\mathscr{V}_A$ and $\Delta\mathscr{V}_B$ are, to a first approximation, neglected (approximation 1); α_A^1, α_A^2, α_B^1 and α_B^2 are the thermal expansion coefficients and χ_A^1, χ_A^2, χ_B^1 and χ_B^2 the isothermal compressibilities.

A perfect solution in equilibrium with crystals of a pure compound (approximations 2) has a concentration given by the Le Chatelier–Schröder relations.[6,7] The crossing of the two solubility curves of the two components is the eutectic point at temperature T_E. The volume of a system comprising at this equilibrium of three phases: crystals (phases 1 and 3) of pure compounds and a perfect solution 2 is:

$$V = n(1-C)\left[\left(\frac{C}{1-C} - \frac{\chi_A^2}{1-\chi_A^2}\right)\mathscr{V}_A^1 + \frac{\chi_A^2}{1-\chi_A^2}\mathscr{V}_A^2 + \mathscr{V}_B^2\right]$$

or in terms of C and C_E

$$V = n\left\{\frac{C_E}{1-C_E}\Delta\mathscr{V}_A\left(\frac{n_B^2}{n}\right) + C\mathscr{V}_A^1 + \Delta\mathscr{V}_B\left(\frac{n_B^2}{n}\right) + (1-C)\mathscr{V}_B^3\right\}$$

with $\chi = n_B^2/n$ and $n = n_A^1 + n_A^2 + n_B^2 + n_B^3$.

Neglecting the temperature, pressure and mole fraction dependence of C_E (approximation 3), the volume variation is

$$dV = n\left\{\left[\frac{C_E}{1-C_E}\Delta\mathscr{V}_A + \Delta\mathscr{V}_B\right]d\chi\right.$$
$$+\left[C\alpha_A^1\mathscr{V}_A^1 + (1-C)\alpha_B^3\mathscr{V}_B^3\right]dT$$
$$\left.-\left[C\chi_A^1\mathscr{V}_A^1 + (1-C)\chi_B^3\mathscr{V}_B^3\right]dP\right\} \qquad (3)$$

Moreover, the temperature-pressure dependence of the eutectic point is given by the relation,

$$\left(\frac{dP}{dT}\right)_e^E = \frac{n_A^E \Delta\mathscr{H}_A + n_B^E \Delta\mathscr{H}_B}{T_E\left(n_A^E \Delta\mathscr{V}_A + n_B^E \Delta\mathscr{V}_B\right)} \tag{4}$$

due to van Laar[8] with n_A^E and n_B^E respectively the numbers of moles of each compound at the eutectic point.

Thermobarograms for crystals melting and crystals dissolution in a fluid phase

For mesogens enclosed in a steel cell, the dilatation with temperature and pressure of the cell can be neglected.[1] For crystal melting of a binary mixture in a fluid phase—for instance a mesophase (M)—with the following approximations:
—for both crystalline phases, the thermal expansion coefficients, isothermal compressibilities and molar volumes have practically the same values[9] (approximation 4)
—the coefficient $(dP/dT)_e^E$ is very near the Clapeyron slope of pure compounds, for instance B,
the relations (3) and (4) give

$$dP = \frac{\dfrac{\Delta\mathscr{V}_B^{KM}}{\mathscr{V}_B^K}}{\alpha_B^K(1 - C_E)\left[\dfrac{\chi_B^K}{\alpha_B^K} - \dfrac{T_B^{KM}\Delta\mathscr{H}_B^{KM}}{\Delta\mathscr{V}_B^{KM}}\right]} d\chi;$$

then, neglecting, as for calculations of thermobarograms of pure compounds,[1] the pressure-temperature dependence of all the quantities in that relation (approximation 5) as: $0 > \chi > 1 - C$

$$(\Delta P_F) = \frac{1}{\alpha_B^K}\frac{\Delta\mathscr{V}_B^{KM}}{\mathscr{V}_B^K}\left[\frac{1}{\dfrac{\chi_B^K}{\alpha_B^K} - \dfrac{T_B^{KM}\Delta\mathscr{V}^{KM}}{\Delta\mathscr{H}_B^{KM}}}\right]\frac{1 - C}{1 - C_E}$$

For the dissolution of an excess of crystals of compound A (phase K) in a fluid phase, for instance a mesophase, $\chi_A^K = 1$ and $\chi_B^K = 0$. Using for the K and M phase, the approximations 1 and 3, the

relations (1) and (2) give

$$dP = \frac{\frac{1}{\alpha_A^K}\frac{\Delta\mathcal{V}_A^{KM}}{\mathcal{V}_A^K}\frac{1-C}{(1-\chi_A^M)^2} + \frac{RT^2}{\Delta\mathcal{H}_A^{KM}}\frac{1}{\chi_A^M}}{\frac{\chi_A^K}{\alpha_A^K} - \frac{T\Delta\mathcal{V}_A^{KM}}{\Delta\mathcal{H}_A^{KM}}} d\chi_A^M \qquad (5)$$

To a first approximation, for a crystal dissolution occurring over a short range of temperature, the pressure-temperature dependence on T can be neglected and then $T \cong T_A^{KM}$ (approximation 6) and using for the last relation the approximation 5, as: $C_E < \chi_A^2 < C$

$$(\Delta P)_{KM} = \frac{\frac{1}{\alpha_A^K}\left(\frac{C-C_E}{1-C_E}\right)\frac{\Delta\mathcal{V}_A^{KM}}{\mathcal{V}_A^K} + R\frac{(T_A^{KM})^2}{\Delta\mathcal{H}_A^{KM}}\ln\frac{C}{C_E}}{\frac{\chi_A^K}{\alpha_A^K} - \frac{T_A^{KM}\Delta\mathcal{V}_A^{KM}}{\Delta\mathcal{H}_A^{KM}}}$$

The slope of the thermobarograms for the crystal dissolution is obtained from relations (1) and (5) and with approximation 6:

$$\left(\frac{dP}{dT_{KM}}\right) = \frac{\alpha_A^K + \frac{\Delta\mathcal{V}_A^{KM}}{\mathcal{V}_A^K}\frac{\chi_A^M(1-C)}{(1-\chi_A^M)^2}\frac{\Delta\mathcal{H}_A^{KM}}{R(T_A^{KM})^2}}{\chi_A^K + \frac{(\Delta\mathcal{V}^{KM})^2}{\mathcal{V}_A^K RT_A^{KM}}\frac{\chi_A^M(1-C)}{(1-\chi_A^M)^2}}.$$

We can show that the slope is positive, and using the approximation 6, at the beginning of the dissolution $(dP/dT)_{KM}$ is smaller than $(dP/dT)_e^E$, and during all the transition, $(dP/dT)_{KM}$ increases. Away from the transitions, for pure compounds, the slope of the thermobarograms is α/χ.[1] For mixtures, with approximation 3, this last relation is still convenient.

The drawing of thermobarograms for melting and excess dissolution of a crystal in a mesophase of binary mixture is given in Figure 2. Typically, for middle values for α, χ and $(dP/dT)_e$ (respectively $8.10^{-4}°C^{-1}$, $8.10^{-10}m^2N^{-1}$, 40 bars K^{-1} for pure compounds), for C

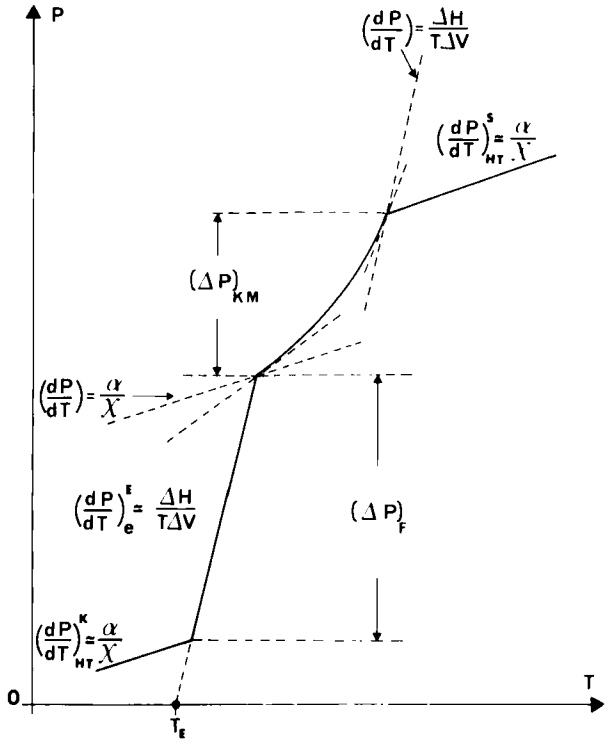

FIGURE 2 Thermobarograms for crystal melting and crystal dissolution in a mesophase of a binary mixture of mesogens.

and C_E, respectively 0.9 and 0.65, and with a 5% relative volume change, the melting pressure increment is 238 bars. With a 15 cm^3 $mole^{-1}$ volume change for the pure compound melting at 300K, the pressure increment for the crystal dissolution is 768 bars. The slope out of the transitions is 10 bars K^{-1} and for the melting mixture 40 bars K^{-1}; the slope increases from 15 bars K^{-1} to 33 bars $^{-1}$ during the crystals dissolution. Then, melting and dissolution of crystals in a mesophase are easily detectable phenomena.

Thermobarograms for transitions between two fluid phases

Using, for transitions between two fluid phases—for instance a mesophase (M) and a liquid phase (I)—of a binary mixture, the approximation 3, and when the enthalpy and volume changes at the transformation respectively for both compounds have practically the same

values (approximation 7), the relations (1) and (2) give:

$$dP = \left\{ \frac{RT^2 \dfrac{\Delta \mathscr{V}_A^{MI}}{\Delta \mathscr{H}_A^{MI}}}{\Delta \mathscr{V}_A^{MI}\left[\dfrac{\chi_A^M}{\alpha_A^M} - \dfrac{T\Delta V_A^{MI}}{\Delta \mathscr{H}_A^{MI}} \right]} \frac{\chi_A^M - \chi_A^I}{\chi_A^I (1 - \chi_A^I)} \right.$$

$$\left. + \frac{\dfrac{\Delta \mathscr{V}_A^{MI}}{\mathscr{V}_A^M}}{\alpha_A^M \left[\dfrac{\chi_A^M}{\alpha_A^M} \dfrac{T\Delta \mathscr{V}_A^{MI}}{\Delta \mathscr{H}_A^{MI}} \right]} \frac{C - C\chi_A^M - C\chi_A^I + \chi_A^M \chi_A^I}{\chi_A^I (1 - \chi_A^I)(\chi_A^M - \chi_A^I)} \right\} d\chi_A^I \quad (6)$$

For compounds where T_A^{MI} is very near to T_B^{MI} (horizontal coexisting curves, the spindle width is very narrow[10] and in the last relation T_A^{MI} can take the place of T (approximation 7). At constant pressure[11]:

$$\frac{\chi_A^M}{\chi_A^I} = \exp\left[\frac{\Delta \mathscr{H}_A^{MI}}{R} \left(\frac{1}{T} - \frac{1}{T_A^{MI}} \right) \right] = \exp[\lambda]$$

For a mixture enclosed in a cell, at the beginning of the transformation $\chi_A^M = C$ and

$$\chi_A^I = C \exp\left[-\frac{(\Delta \mathscr{H}_A^{MI})_i}{R} \left(\frac{1}{T^i} - \frac{1}{T_A^i} \right) \right]$$

(i as initial), and at the end of the transformation

$$\chi_A^I = C \quad \text{and} \quad \chi_A^M = C \exp\left[\frac{(\Delta \mathscr{H}_A^{MI})_f}{R} \left(\frac{1}{T^f} - \frac{1}{T_A^f} \right) \right]$$

(f as final). For not too high pressures,

$$(\Delta \mathscr{H}_A^{MI})_i \cong (\Delta \mathscr{H}_A^{MI})_f [12]$$

and for $\frac{1}{T^i} - \frac{1}{T_A^i} \cong \frac{1}{T^f} - \frac{1}{T_A^f}$ (approximation 8)

$$(\Delta P)_{MI} = \frac{\frac{1}{\alpha_A^M}\frac{\Delta \mathscr{V}_A^{MI}}{\mathscr{V}_A^M} U_{MI} + \frac{R(T_A^{MI})^2}{\Delta \mathscr{H}_A^{MI}} W_{MI}}{\frac{\chi_A^M}{\alpha_A^M} - \frac{T_A^{MI}\Delta \mathscr{V}_A^{MI}}{\Delta \mathscr{H}_A^{MI}}}$$

with

$$U_{MI} = \left[\frac{C(1-\chi_A^M)}{\chi_A^M} \ln \chi_A^I - \frac{\chi_A^M(1-C)}{\chi_A^M - 1} \ln(1-\chi_A^I) \right.$$

$$\left. - \frac{2C\chi_A^M - C - (\chi_A^M)^2}{\chi_A^M(\chi_A^M - 1)} \ln(\chi_A^M - \chi_A^I) \right]_{\chi_A^M = C; \chi_A^I = C\exp[-\lambda]}^{\chi_A^M = C\exp\lambda; \chi_A^I = C}$$

and

$$W_{ML} = [\chi_A^M \ln \chi_A^I - (\chi_A^M - 1)\ln(1 - \chi_A^I)]_{\chi_A^M = C; \chi_A^I = C\exp[-\lambda]}^{\chi_A^M = C\exp[\lambda]; \chi_A^I = C}$$

The slope of the thermobarogram for mesophase-liquid transformation is obtained from relation (1) and (6) and with approximation 7

$$\left(\frac{dP}{dT_{MI}}\right) = \frac{\alpha_A^M + \frac{\Delta \mathscr{V}_A^{MI}}{\mathscr{V}_A^M} \frac{(C - C\chi_A^M - C\chi_A^I + \chi_A^M\chi_A^I)\Delta \mathscr{H}_A^{MI}}{(\chi_A^M - \chi_A^I)^2 R(T_A^{MI})^2}}{\chi_A^M + \frac{(C - C\chi_A^M - C\chi_A^I + \chi_A^M\chi_A^I)}{(\chi_A^M - \chi_A^I)^2} \frac{(\Delta \mathscr{V}_A^{MI})^2}{\mathscr{V}_A RT_A^{MI}}}$$

That slope is positive, and for horizontal coexisting curves, always bigger than α/χ (slope out of the transition) and smaller than $(dP/dT)_e^{MI}$. When the width of the spindle is bigger at the beginning of the transformation than at the end of it, the slope at the beginning is smaller than at the end and conversely. For a spindle width smaller than 1%, the slope at the mesophase-liquid transition is practically a

constant and very near to the Clapeyron slope of pure compounds; for a 10% spindle width, the slope decreasing is 8%. Moreover, the variation with concentration of $(dP/dT)_{MI}$ is very small. For horizontal coexisting curves, using the previous data for $\alpha, \chi, (dP/dT)_e$ and C, the pressure increments $(\Delta P)_{MI}$ for a nematic–smectic A transition ($\Delta\mathcal{H} \cong 0.01$ kcal mol^{-1}, $\Delta\mathcal{V} \cong 0.04$ cm^3 mol^{-1}, $\Delta\mathcal{V}/\mathcal{V} \cong 0.01\%$), nematic–liquid or smectic C–nematic transition ($\Delta\mathcal{H} \cong 0.1$ kcal mole^{-1}, $\Delta\mathcal{V} \cong 0.4$ cm^3 mole^{-1}, $\Delta\mathcal{V}/\mathcal{V} \cong 0.1\%$) for a transition between a very organized mesophase and a smectic or nematic phase ($\Delta\mathcal{H} \cong 1$ kcal mole^{-1}, $\Delta\mathcal{V} \cong 4$ cm^3 mole^{-1}, $\Delta\mathcal{V}/\mathcal{V} \cong 1\%$) or for a transition between two organized mesophases ($\Delta\mathcal{H} \cong 5$ kcal mole^{-1}, $\Delta\mathcal{V} \cong 20$ cm^3 mole^{-1}, $\Delta\mathcal{V}/\mathcal{V} \cong 5\%$) are respectively 20 bars, 30 bars, 40 bars and 150 bars. Then, transitions between fluid phases of binary mixtures are phenomena easily detectable by the metabolemeter.

4. EXPERIMENTS

Apparatus and experimental procedures for the detection of first and second order phase transitions for pure compounds are previously described[1,3] and are here extended to phase transitions of binary mixtures.

First experiments were performed to verify that the metabolemeter is convenient to detect phase transitions of binary mixtures of mesogens and to deduce the isobaric phase diagrams. To simplify, compounds exhibiting only one mesophase and transitions near room temperature were selected. The 4-methoxy-4′-ethyltolane (MET),

MET

and 4-methoxy-4′–nonyltolane (MNT)

MNT

are convenient[13] (transition data in Table I). The isobaric phase diagram for these compounds is known[14] (Figure 3). The virtual nematic-liquid transition temperature of MET was determined by the droplets method[17]; the other transition temperatures were obtained by the contact method[18]; the eutectic and liquid apparition point concentrations are only calculated data[19]. Beyond the two pure tolanes, we have studied the phase transitions for two mixtures: the first, near to 10 mole %—to observe melting, crystal dissolution in the nematic and

nematic-liquid (N-I) transition (spindle)—and the second, near to 70 mole %—to observe melting, crystal dissolution in the nematic, N-I transition and crystal dissolution in the liquid.

The following experiments were made to verify the existence of an unknown mesophase which appears in the binary mixtures of bis-(4-4′-n-heptyloxy benzylidene)-1,4-phenylenediamine (HBPD)

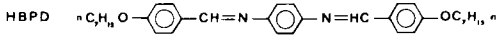

and −1 − (methyl)-heptyl terephthalidene bis amino cinnamate (MHTAC)

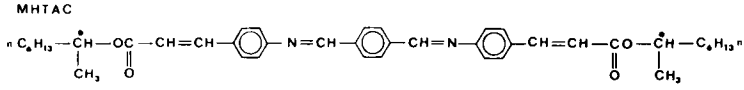

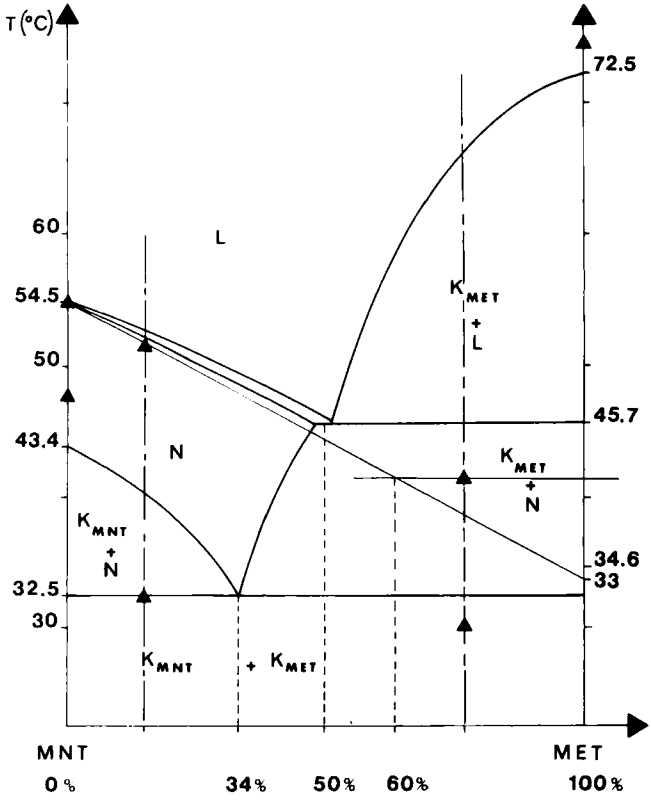

FIGURE 3 Isobaric phase diagram for methoxy-ethyltolane (MET) and methoxy-n-nonyltolane (MNT): full and dashed lines: Domon, (Ref. 14) ▲: this work.

TABLE I

Literature data for the temperature T (°C), Clapeyron slope $(dP/dT)_e$ (bars K^{-1}), enthalpy $\Delta\mathcal{H}$ (kcal mole^{-1}) and volume $\Delta\mathcal{V}$ (cm^3 · mole^{-1}) changes for the transitions of: 4-Methoxy-ethyltolane (MET): I_a 4-Methoxy-4′-nonyltolane (MNT): I_b Bis-(4-4′-n-heptyloxybenzylidene)-1,4-phenylene diamine (HBPD): I_c 1 (Methyl)-heptyl terephthalidene bis amino cinnamate (MHTAC): I_d

I_a	K	N	I	REFERENCES
T	• 72,5		•	13
		• (34,6)[a] •		14
ΔH	5,62			15
		(0,17)[a]		14

I_b	K	N	L	REFERENCES
T	• 41	• 53,5	•	13
	• 43,4	• 54,5	•	14
ΔH	7,45	0,214		13
$(\frac{dP}{dT})_e$	43,5	41,6		16
ΔV	22,8	0,65		16

I_c

	K_1	K_2	K_3	K_4	S_K	S_J	S_I	S_C	N	I	REFERENCES
T	. 117 . 112	. 127 . 125,4	.[130] .	. 146 . 148,5	. 154 . 155,9	. 157 . 162,7	. 164 . 168,2	. 197 . 198	. 241 . 240,4	.	20 21
ΔH	3,42 3,04	1,42 1,24	0,06	2,68 1,63	0,51 0,36	0,12	0,77 0,76[b]	0,86 0,65	0,51 0,26		22 21
$(\frac{dP}{dT})_e$	30	14,5		24,1	29,1	23	24,3	28,7	19,4		21
ΔV	11	9		6,7	1,2 0,99	3[b] -1,52	3	2	1,6		21 23

I_d

	K_1	K_2	S_0	S_Q	L	REFERENCES
T	. 88	. 95	. 130	. 133	.	24
ΔV	0,95	4,02	0,285	0,097		24

a : virtual transition

b : S_J- S_C transition

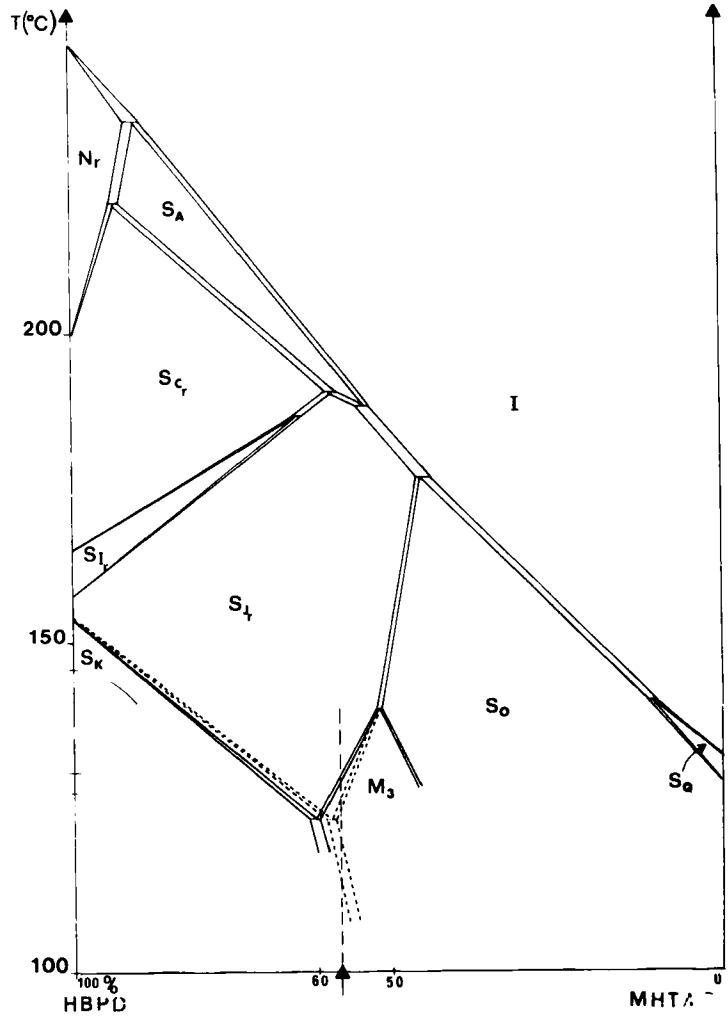

FIGURE 4 Isobaric phase diagram for bis-(4-4'-n-heptyloxybenzylidene)-1, 4-phenylenediamine (HBPD) and 1 (methyl)-heptyl terephthalidene bis amino cinnamate (MHTAC): full lines: microscopic observations, dashed lines: metabolemeter.

(transition data for pure compounds in table I). The isobaric phase diagram of both compounds has been studied from microscopic observations with the contact method.[18] Between 115°C and 125°C in the middle of the phase diagram, an intermediary phase called M_3 appears (Figure 4). To verify that M_3 is a new mesophase, X ray studies are necessary; but the contact method does not give precisely the concentration domains of the phases. DTA studies had been

performed[25] but no improvement to the thermograms was possible. So it was interesting, first to verify the M_3 existence and second, to specify its range of concentration existence with the metabolemeter.

5. RESULTS

MET-MNT phase diagram

Figure 5 and 6 give experimental thermobarograms obtained on heating for pure MET and MNT (1.2 mg samples). The transition temperatures under atmospheric pressure, slopes out and at the transition are reported in Table II. The molar volume change under atmospheric pressure is calculated from the Clapeyron relation and calorimetric data for enthalpy changes and transition temperatures (Table II).

For a mixture of 11.9% by mass of MET (Img sample), figure 7a gives experimental thermobarograms obtained on heating. The melt-

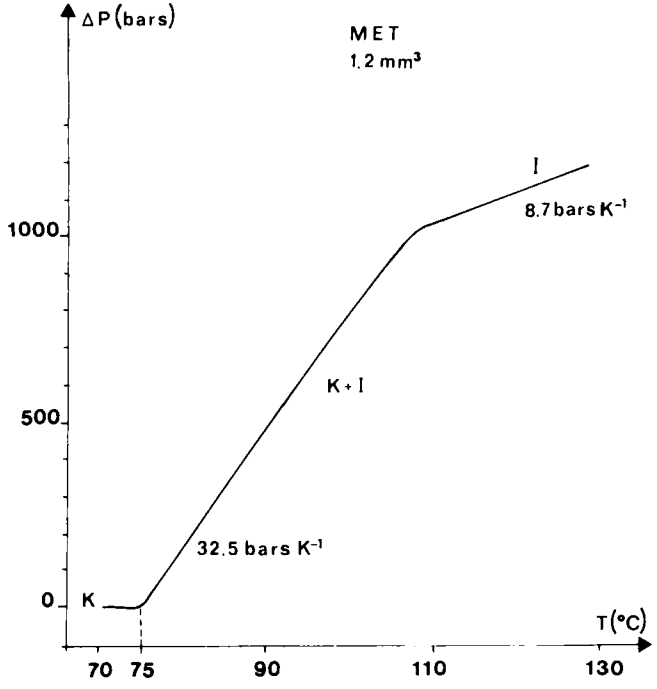

FIGURE 5 Experimental thermobarogram showing, for a 1.2 mm^3 sample, the melting for MET.

TABLE II

Calculated and experimental data for the temperature T (°C), Clapeyron slope $(dP/dT)_e$ (bars K^{-1}), volume change $\Delta\mathcal{V}$ (cm^3 mole^{-1}) and slope out of the transition α/χ (bars K^{-1}) for MET (II_a), MNT (II_b), HBPD (II_c) and MHTAC (II_d).

II_a	K	N	L
T	• 75	• (32,5)[a]	• •
$(\frac{dP}{dT})_e$	32,5		
ΔV	20,92	0,85[b]	
$\frac{\alpha}{\chi}$			8,7

II_b	K	N	L
T	• 48	• 56	•
$(\frac{dP}{dT})_e$	46,4	31,9	
ΔV	21,37	0,85	
$\frac{\alpha}{\chi}$		13,6	11,6

II_c	K_1	K_2	K_3	K_4	S_K	S_J	S_I	S_C
T	• 110,7	• 126	•	• 147,3	• 153,8	• 162,4	• 168,6	•
$(\frac{dP}{dT})_e$	27,2	20	17[c]	29,7	22	18,8	21,2	
ΔV			0,35[c]			0,80	1,85	
$\frac{\alpha}{\chi}$	16,7			12,4	13,7	9,6	11,9	8,6

II_d	K_2	K_1	S_0	S_Q	I
T	• ∿ 84	• ∿ 94	•	•	•
$(\frac{dP}{dT})_e$	18	19	22,5		
ΔV	6,1	24	1,3		
$\frac{\alpha}{\chi}$	8	6	6,5	5,5	

a : Virtual transition temperature obtained by extrapolation on isobaric phase diagram.

b : Calculated data from relation 4.

c : monotropic K_3- K_4 transition

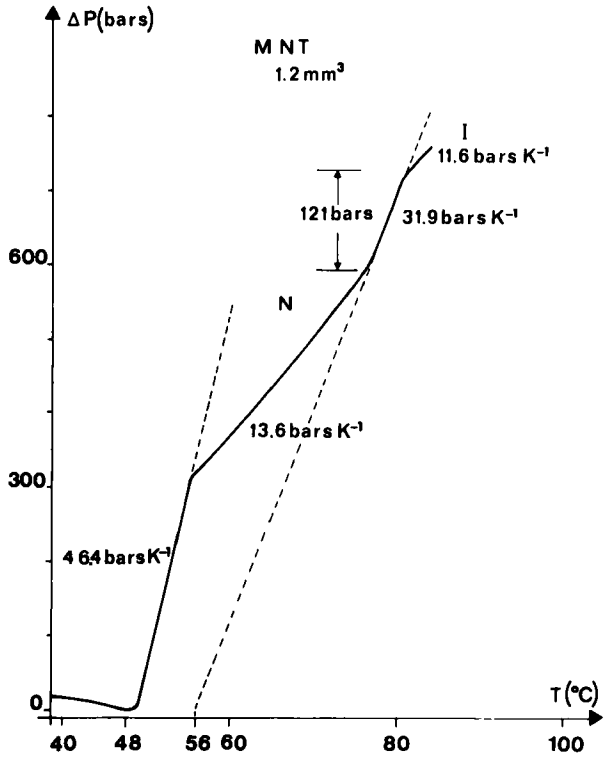

FIGURE 6 Experimental thermobarogram showing, for a 1.2mm^3 sample, the melting and nematic-liquid transition for MNT.

ing appears at 32°C under atmospheric pressure, and the N-I transition at 63.5°C under 500 bars. The curve between melting and clearing is, first of all, the MNT crsytal dissolution and then, nematic dilatation. At 60°C and under 450 bars a faint charge of slope appears corresponding to the end of the dissolution and the beginning of the nematic dilatation; but the slope change is faint and this interpretation is uncertain. Figure 7b shows the N-I transition detected under low pressure and for a slow speed for heating (1°C min^{-1}). The transition temperature extrapolated under atmospheric pressure is 52°C which agrees with literature data.

For a mixture of 71.9% by mass of MET (0.8 mg sample), figure 8a and b give experimental thermobarograms obtained on heating. In figure 8a, the melting (that appears at about 30°C under atmospheric pressure), MET crystal dissolution in the nematic, N-I tran-

sition (slope about 16 bars K^{-1}) and finally MET crystal dissolution in the liquid are successively observable. Figure 8b gives the upper part of the thermobarogram and shows the N-I transition and crystal dissolution in the liquid.

Experimental points obtained with the metabolemeter are reported on the phase diagram (Figure 3). For the 11.9% mixture the temperature of the N-I transition and the melting agree with contact method results. For the 71.9% mixture, for the N-I transition temperature a 5°C difference exists, which can be explained by uncertainties in our measurements (the transition temperature under atmospheric pressure was obtained with only two points). Then, the concentration for the liquid appearance point is 60% and differs from the calculated value (50%). The virtual nematic-liquid transition temperature of MET obtained with the metabolemeter is 33°C and agrees with droplets method result.

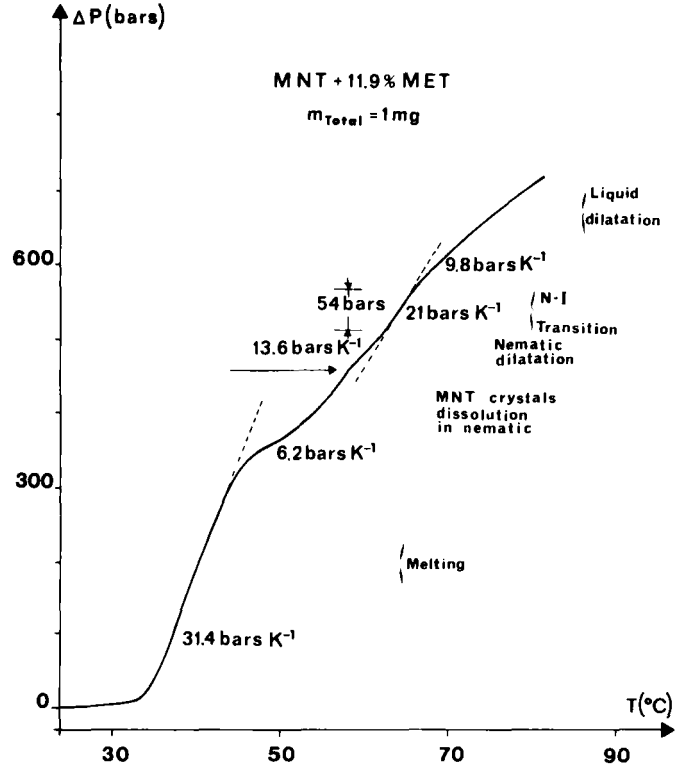

FIGURE 7 (a)

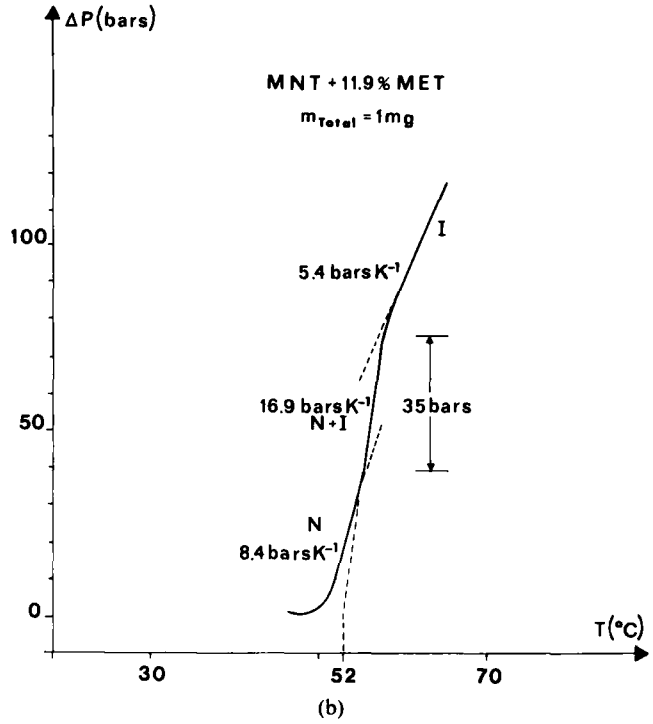

FIGURE 7 Experimental thermobarograms for an MET-MNT mixture with 11.9% by mass of MET (1 mg sample), obtained on heating, and showing, a: the different transformations, b: the nematic-liquid transition obtained for a slow speed of heating.

HBPD-MHTAC phase diagram

The studies with the metabolemeter of pure HBPD are published elsewhere.[3] For pure MHTAC, figure 9a and b give experimental thermobarograms showing the $K_1 - K_2$, $K_2 - S_0$ and $S_0 - S_Q$ transitions. In figure 9b a slope change is detected at 180°C under 620 bars pressure, corresponding to the $S_Q - I$ transition (weakly first order phase transition: $\Delta\mathcal{H} = 0.097$ kcal mole^{-1} under atmospheric pressure). But the slope changes are very small and this interpretation is uncertain. The P-T phase diagram of MHTAC is given in figure 10. The slopes out of the transitions and the Clapeyron slopes are reported in table II. The volume changes are calculated from the Clapeyron relation using the data of table I and II and reported in table II. For evidence of the M_3 phase, figure 4 suggests the study of a mixture between 50 and 60 mole % of HBPD. For a 58 mole %

mixture (0.8 mg sample) an experimental thermobarogram, obtained on heating is given in Figure 11: two transitions are observable at low temperature. From several thermobarograms, obtained from several fillings of the cell, the P-T phase diagram can be drawn for the studied concentration (figure 12): an M_3 intermediary phase occurs between the S_K and S_J phase under atmospheric pressure between 113 and 124°C. The isobaric phase diagram is drawn in figure 4 to satisfy the experimental points obtained with the metabolemeter.

6. DISCUSSION

For both MET and MNT mixtures, experimental thermobarograms agree with estimated ones. The melting and N-I transition are easily

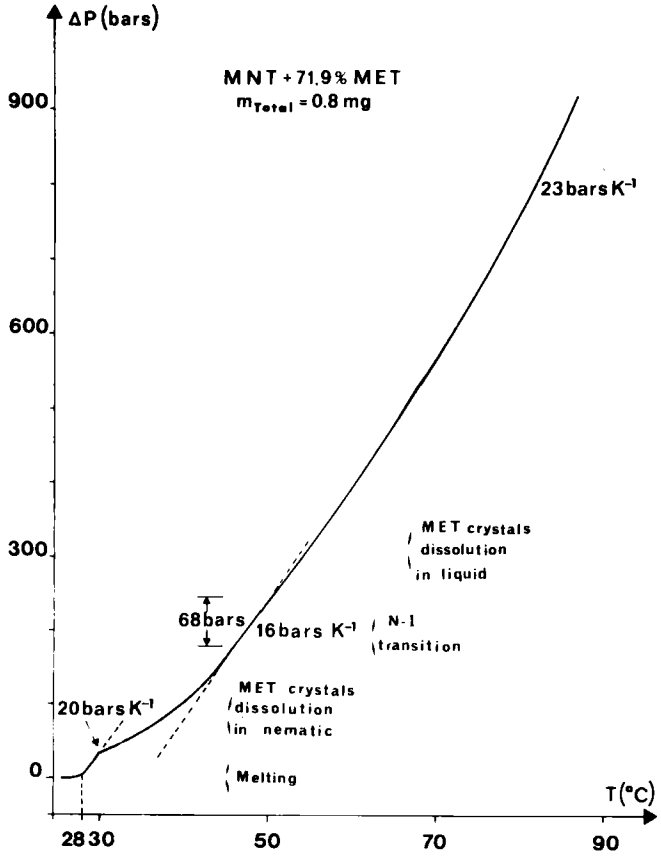

FIGURE 8 (a)

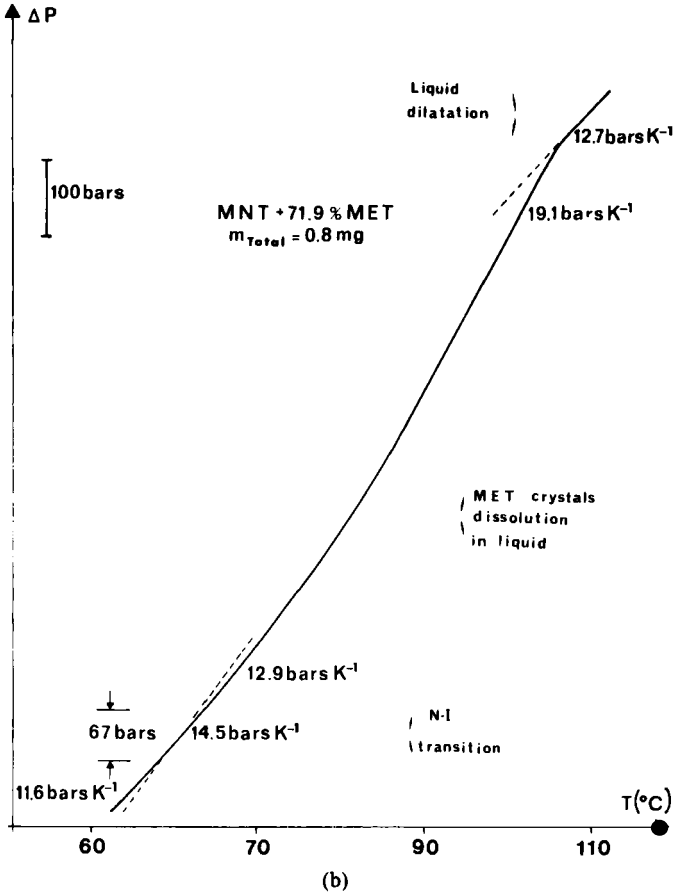

FIGURE 8 Experimental thermobarograms for an MET-MNT mixture with 71.9% by mass of MET (0.8mg sample), obtained on heating, and showing, a: the different transformations, b: the nematic-liquid transition, MET crystal dissolution in the liquid and liquid dilatation.

detectable and the transition temperatures can be deduced from thermobarograms. The slopes for the melting have the same order of magnitude as the Clapeyron slopes of pure compounds (about 35 bars K^{-1}). The N-I transition slopes can be considered as a constant. The slopes for the nematic and liquid phase are near to α/χ for pure mesogens (about 10 bars K^{-1}), and during the crystal dissolution the slope always increases.

The temperatures for the end of the crystal dissolution in the first case (11.9% MET mixture) have not been determined precisely, and in the second case (71.9% MET mixture) they can't be determined under a different pressure (a failure occurred during the first recording). The extrapolation under atmospheric pressure was not possible, which prevents the determination, from the solubility curve of the concentration at the eutectic and liquid appearance points. No calculation is possible to compare the experimental and calculated pressure increment data because no literature data is known. Finally, from relation (4) the volume change for pure compounds can be

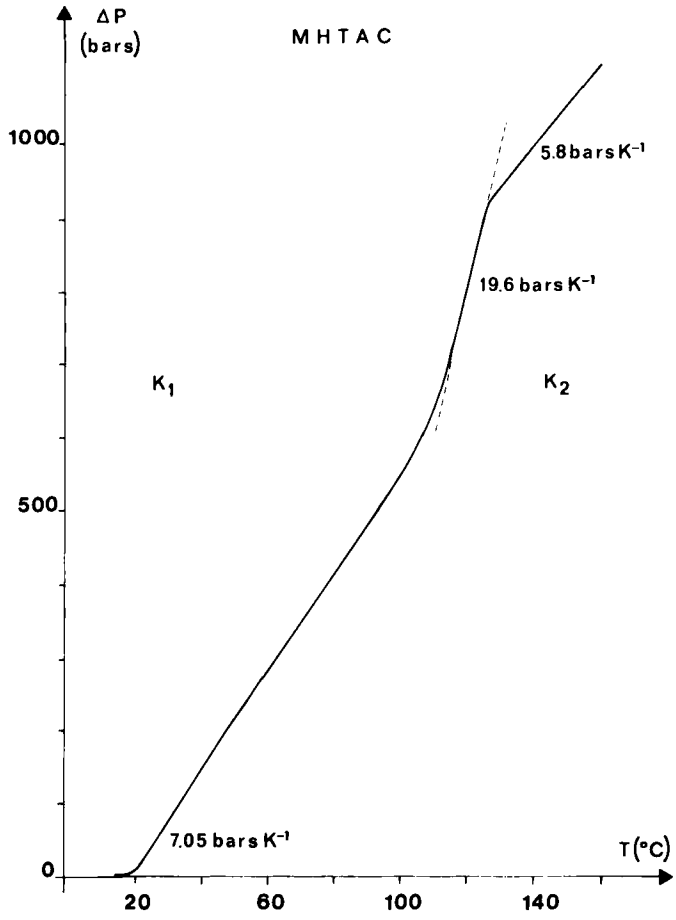

FIGURE 9 (a)

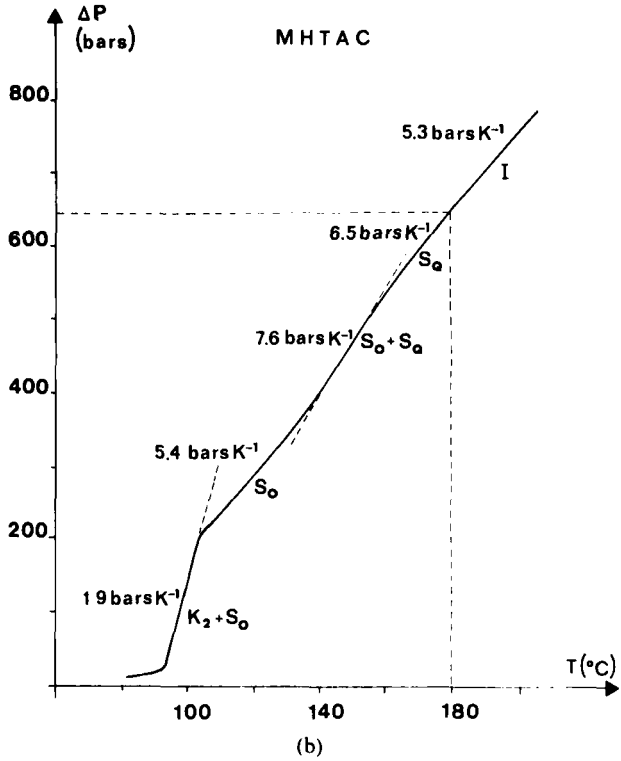

FIGURE 9 Experimental thermobarogram for MHTAC, obtained on heating and showing a: the $K_1 - K_2$ transition, b: the $K_2 - S_0$, $S_0 - S_Q$ (and perhaps $S_Q - I$) transitions.

deduced

$$\Delta\mathscr{V}_B = \frac{\frac{\chi_A^E}{\chi_B^E}\Delta\mathscr{H}_A + \Delta\mathscr{H}_B}{T_E\left(\frac{dP}{dT}\right)_e^E} - \frac{\chi_A^E}{\chi_B^E}\Delta\mathscr{V}_A$$

The volume change for the virtual nematic-liquid transition, using the data of table I and II and 0.5 for x, is 0.85cm^3 mole^{-1}.

For the studied mixture of HBPD and MHTAC, the results obtained with the metabolemeter confirm, and state precisely, the contact method observations about the M_3 phase existence. The mesophase takes place between the S_K and S_J phase; so it seems that M_3 is a new smectic phase. X ray studies are necessary to determine the structure.

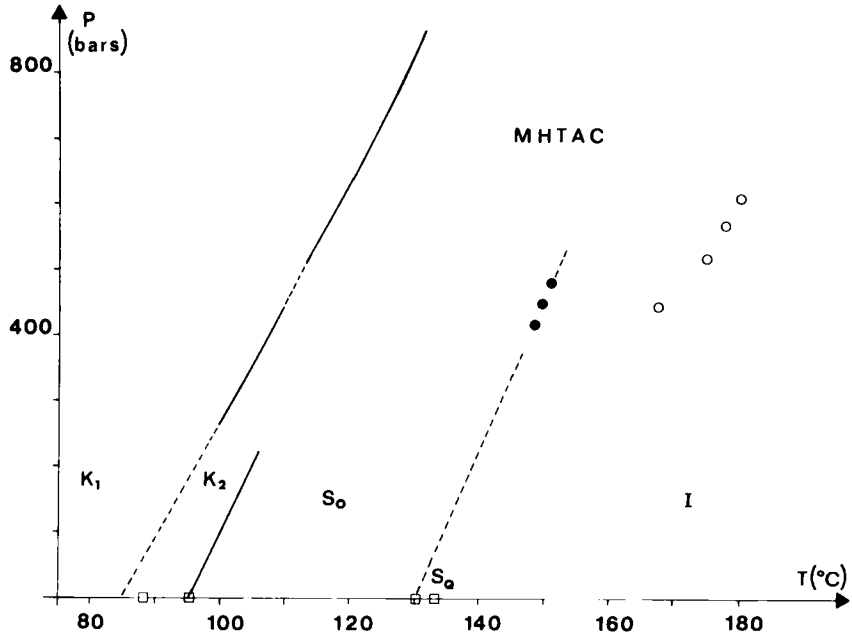

FIGURE 10 Pressure-temperature phase diagram for MHTAC, □: Levelut and al. (Ref. 24), ●: transition temperature under pressure taken at the middle of the experimental equilibrium curves, ○: transition temperature under pressure measured at the change of slope of thermobarograms.

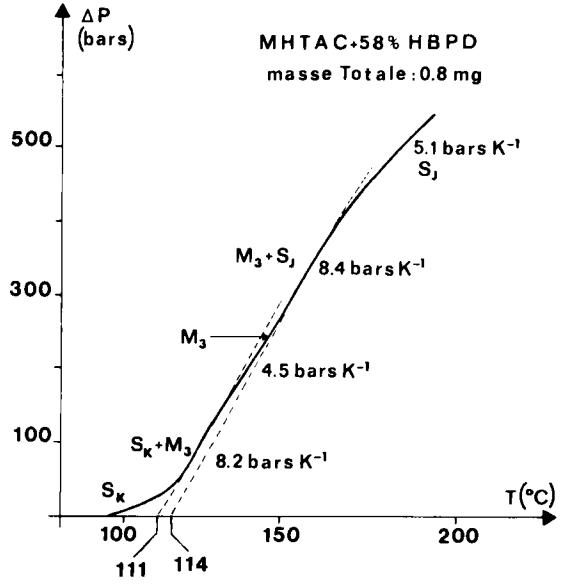

FIGURE 11 Experimental thermobarograms, obtained on heating and showing the $S_K - M_3$ and $M_3 - S_J$ transitions for a HBPD-MHTAC mixture with 58 mole% of HBPD (0.8mg sample).

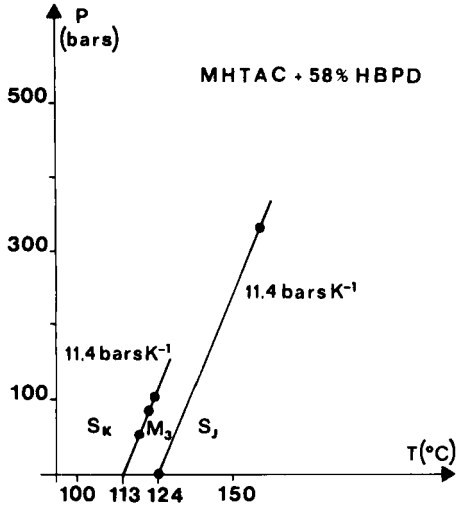

FIGURE 12 Pressure-temperature phase diagram for a HBPD-MHTAC mixture with 58 mole % of HBPD.

7. CONCLUSION

Phase transitions of pure mesogens can be detected by the measurement versus temperature of the pressure of a sample enclosed in a metallic cell. This method has been applied for the detection of transitions in binary mixtures. Thermobarograms for crystal melting, crystal dissolution in a fluid phase and transitions between two fluid phases of binary mixtures have been calculated. Experimental tests have been performed on two binary mixtures of 4-methoxy-4′-ethyltolane and 4-methoxy-4′-nonyltolane. The thermobarograms obtained agree with calculations and allow the determination, for the eutectic point and liquid appearance point, of the transition temperature under atmospheric pressure. Moreover the volume change for the virtual nematic-liquid transition has been deduced. Finally the study by this method of a binary mixture of (1-methyl)-heptyl terephthalidene bis amino cinnamate and bis 4-n heptyloxybenzylidene phenylene diamine has allowed the confirmation of microscopic observations on the existence of an intermediary phase which doesn't exist for pure compounds, and determined precisely its concentration domain.

Acknowledgments

The authors are grateful, for the synthesis of Tolanes to J. Jacques, J. Malthete, M. Leclercq, M. Dvolaitzky, J. Gabard, V. Pontikis, for the synthesis of HBPD to L. Liebert and C. Germain, for the synthesis of MHTAC to P. Keller.

References

1. J. M. Buisine, B. Soulestin and J. Billard, *Mol. Cryst. Liq. Cryst.* **91**, 115 (1983).
2. J. M. Buisine, B. Soulestin and J. Billard, *Mol. Cryst. Liq. Cryst.* **97**, 397 (1983).
3. J. M. Buisine, *Mol. Cryst. Liq. Cryst.* **109**, 143 (1984).
4. J. M. Buisine, P. Le Barny and J. C. Dubois, *J. Polym. Sci.: Polym. Lett.* **22**, 149 (1984).
5. For detailed calculations see J. M. Buisine, Thèse, Lille (1984).
6. H. Le Chatelier, *C. R. Acad. Sci. Paris* **100**, 50 (1885).
7. I. Schröder, *Z. phys. Chem.* **11**, 441 (1893).
8. I. Prigogne and R. Defay, *Thermodynamique chimique* (Dunod, Paris, 1950).
9. A. Beguin, J. Billard, F. Bonamy, J. M. Buisine, P. Cuvelier, J. C. Dubois, and P. Le Barny, *Sources of Thermodynamic Data on Mesogens* (To appear).
10. M. Domon, Thèse, Lille (1973).
11. J. J. van Laar, *Arch. Neerl. Sci. Exates Nature* **118**, 267 (1903), *Z. phys. Chem.* **63**, 266 (1908), *Z. phys. Chem.* **64**, 257 (1908).
12. See for example W. Spratte and G. M. Schneider, *Ber. Bunsen Ges.* **80**, 886 (1976).
13. J. Malthete, M. Leclercq, M. Dvolaitzky, J. Gabard, J. Billard, V. Pontikis and J. Jacques, *Mol. Cryst. Liq. Cryst.* **23**, 233 (1973).
14. M. Domon, Private communication.
15. Unpublished results.
16. L. Liebert, W. B. Daniels and J. Billard, *Mol. Cryst. Liq. Cryst. Lett.* **41**, 57 (1977).
17. J. Malthete and J. Billard, *Mol. Cryst. Liq. Cryst.* **54**, 45 (1979).
18. L. Koffler and A. Koffler, *Thermomikromethoden* (Verlag chemie, Weinheim, 1954).
19. M. Domon and J. Billard, *Pramana suppl N°1* ed. S. Chandrasekhar, 131 (1975).
20. P. A. C. Gane, A. J. Leadbetter, P. G. Wrighton, J. W. Goodby, G. W. Gray, and A. R. Tajbaksh, *Mol. Cryst. Liq. Cryst.* **100**, 67 (1983).
21. W. Spratte and G. M. Schneider, *Mol. Cryst. Liq. Cryst.* **51**, 101 (1979).
22. E. M. Barall, II, J. W. Goodby and G. W. Gray, *Mol. Cryst. Liq. Cryst. Lett.* **49**, 319 (1979).
23. D. Demus and R. Rurainski, *Mol. Cryst. Liq. Cryst.* **16**, 171 (1972).
24. A. M. Levelut, G. Germain, P. Keller, L. Liebert and J. Billard, *J. de Phys.* **44**, 623 (1983).
25. L. Liebert, Private communication.